Dependence of Wave-Breaking Statistics on Wind Stress and Wave Development

Kristina B. Katsaros and Serhad S. Ataktürk

Department of Atmospheric Sciences, University of Washington,
Seattle, Washington 98195.

Summary

Incidence of wave breaking for pure wind driven waves has been studied on Lake Washington at wind speeds up to 8 m s^{-1}. Video recordings were employed to identify and categorize the breaking events in terms of micro–scale, spilling and plunging breakers. These events were correlated with the magnitude of the wave spectrum measured with a resistance wire wave gauge and band pass filtered between 6 and 10 Hz. An equivalent percentage of breaking crests were found for spilling and plunging events.

Wave forcing as measured by wind stress (or friction velocity, u_*, squared) and by inverse wave age, u_*/C_p, where C_p is the phase velocity of the waves at the peak of the frequency spectrum, were found to be good predictors of percentage of breaking crests. When combined in a two parameter regression, those two variables gave small standard deviation and had a high correlation coefficient (66%). The combination of u_*^2 and u_*/C_p can be understood in physical terms. Furthermore, for the larger values of u_*^2 the dependence of wave breaking on wave age was stronger than at the low end of the values for u_*^2 and u_*/C_p. Thus, both the level of wave development as determined by inverse wave age, which we may term *relative wind effectiveness for wave forcing* and the wind forcing on the water surface determine the incidence of wave breaking.

Substituting $U_{10}^{3.75}$ (which is the dependence of whitecap cover found by Monahan and coworkers) an equivalent correlation was found to the prediction by u_*^2. Slightly better standard deviation value and higher correlation coefficient were found by using a Reynolds number as predictor. A two–parameter regression involving u_*^2 and a Reynold's number proposed by Toba and his colleagues (e.g., Toba and Koga, 1986) which relates u_*^2 and peak wave frequency, improves the correlation even more but is less easy to interpret in physical terms.

The equivalent percentage of breaking crests obtained in our previous study (Weissman et al., 1984) was reported at 8.6% for a short record obtained at U_{10N} of about 6 ms^{-1}. Typical values in the current study for similar conditions are 6%, which is consistent with the previous study in view of the scatter. In that study we did not have a video recording system, so the observed breaking may include more of the micro–scale breaking events, and the value, 8.6%, is well within the range of highly probable sampling variability.

INTRODUCTION

Wave breaking can be a dramatic change in sea surface characteristics and occurs on many scales. It plays a significant role in air–sea exchanges of momentum, energy and mass in various ways (e.g., Donelan, 1990; Banner, 1990). In particular, it is the dominant mechanism responsible for wave dissipation; it removes momentum and energy from the wave field and transfers the momentum to surface currents and the energy into both turbulence and currents. The dissipation of wave energy, due

M. L. Banner, R. H. J. Grimshaw (Eds.)
Breaking Waves
IUTAM Symposium Sydney/Australia 1991

to breaking, is one of the key parameters in wave prediction models which are based on the energy transfer equation:

$$\frac{\partial E}{\partial t} + V \cdot \nabla E = S_{in} + S_{nl} + S_{diss} \qquad (1)$$

where E is the wave spectral energy density, V is velocity at which the wave energy propagates (i.e., group velocity plus currents), S_{in} is source function due to wind input, S_{nl} is source function due to nonlinear wave–wave interactions, and S_{diss} is source term due to dissipation. In the state of the art, third generation ocean wave prediction model, the WAM model (the WAMDI Group, 1988), S_{in} based on field measurements has been adopted from that of Snyder et al. (1981), S_{nl} derived on theoretical grounds has been taken from Hasselmann et al. (1985) and, S_{diss} inferred from the residual term in numerical energy balance experiments has the form proposed by Komen et al. (1984). Despite its importance, S_{diss} is the least known of these three source terms.

Whitecaps, which are related to the wave breaking but also includes the more persistent visible foam patch, have been studied extensively by Monahan and coworkers using statistical analysis of photographs and video recordings (e.g., Monahan, 1968, 1971; Monahan and O'Muircheartaigh, 1980; Monahan et al., 1983; O'Muircheartaigh and Monahan, 1986; O'Muircheartaigh et al., 1991). In these studies areal whitecap coverage has been found to correlate with the 10 m neutral wind speed raised to the power 3.75, $U_{10N}^{3.75}$ (also see, Wu, 1979, 1986).

Because of the increased significance of small scale perturbations on the sea surface for the return of incident radar signals and for microwave emissions, renewed interest in defining wave breaking and relating its occurrence to other measurable quantities has developed (e.g., Banner and Fooks, 1985). Jessup et al. (1990, 1991a) and Bush et al. (1991) have related the *sea spikes* in radar return at X, C and Ku bands to wave breaking observed from video records. The latter studies found that sea spikes often occurred without visible breaking events, but Jessup et al. (1991b) comment that the largest spikes in their study were all directly relatable to readily visible plunging breakers (i.e., dramatically breaking wave crests).

The Bragg scatter is the dominant mechanism responsible for the variations in the normalized radar backscatter cross section, σ_o, as a function of wind speed or stress. It is currently recognized that breaking events may modify this relationship, especially since it is unlikely that occurrence of wave breaking has the same dependence on wind speed or stress as the part of the wave spectrum corresponding to Bragg scattering water waves. It has also been observed that wave breaking is related not only to the wind forcing but that details of the underlying sea state must also be considered. Numerous studies have considered the hydrodynamic instability of the water surface itself, i.e., in situations with no atmospheric forcing at all (see other articles in this volume). On theoretical grounds

Phillips (1988) predicted that contributions to σ_o by breaking waves should be proportional to u_*^3, where u_* is friction velocity defined through $\tau_o/\varrho = u_*^2$. τ_o is wind stress at the sea surface and ϱ is air density. Jessup et al. (1990, 1991b) verified this relationship.

Thus, the variability of processes responsible for wave breaking events may also be responsible for some of the scatter found between measured radar cross sections and wind speed (or wind stress). So far as the relationship to wind stress is concerned, it is quite possible that the intensity of wave breaking affects the wind stress in a manner which more closely parallels the effect on radar backscatter than the relationship between 10 m neutral wind speed, U_{10N}, and σ_o. It is customary to use U_{10N} rather than the true wind speed in this relationship. U_{10N} is convertible to a wind stress by defining a relationship between the neutral drag coefficient, C_{DN}, and U_{10N} viz:

$$\tau_o = \varrho\, C_{DN}\, U_{10N}^2 \,. \tag{2}$$

This relationship represents an average condition if typical values for C_{DN} are used (e.g., Smith, 1980; Liu et al., 1979). For anomalous wave breaking a different C_{DN} value should probably be employed and σ_o may be a very good measure of the effective τ_o.

In this study we extend the work of Weissman et al. (1984), who developed a technique for identifying breaking waves from the record of a resistance wire wave gauge. That study was based on a limited time series and only visual observations of the conditions at the wave wire. In this study video recordings were employed.

A preliminary study on sea spikes and wave breaking by Bush et al. (1991) with data obtained on our Lake Washington site has been carried out. Further work on the relationship between wind and wave parameters, frequency of occurrence of wave breaking and radar cross–sections at X, C and Ku bands will be reported elsewhere in the near future.

EXPERIMENTAL SET–UP AND DATA SETS ANALYZED

This work was carried out at our field station on Lake Washington where wind and waves arrive after an over water fetch of 7 *km* (Figure 1.a). A complete suite of environmental measurements was collected, which includes mean wind speed, temperature and humidity at 2 *m* and 8 *m* heights, turbulent fluxes of momentum, heat and water vapor at 8 *m* and wave height from a resistance wire wave gauge hanging from a boom extending 2 *m* upwind of the supporting platform (Figure 1.b). The wave wire was made of stainless steel, 100 μm in diameter.

For the purpose of this study, 10 data sets were analyzed. The length of each data set is 2 hours. The experimental conditions during these data sets are summarized in Table I where for each run the

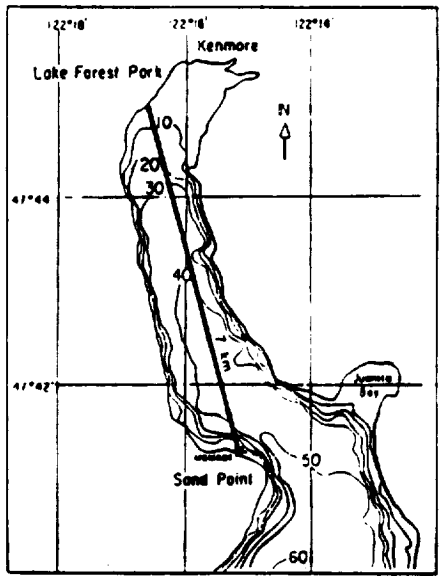

Figure 1a: The location of our field station (MSMAST) on Lake Washington. The tower is 15 *m* offshore and at a depth of 4 *m*. The contours show the water depth in meters.

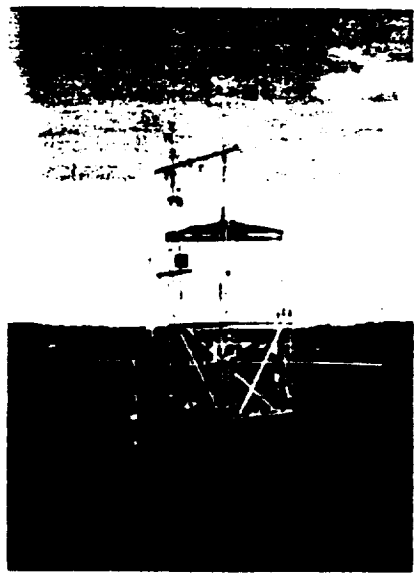

Figure 1b: The Lake Washington tower with meteorological instrumentation, wire wave gauge (at the left most tip of the low level boom) and the video camera (at the lower section of the platform).

mean values (the first line) and the standard deviations (the second line) of various environmental variables are provided.

ANALYSIS

Weissman et al. (1984) defined three types of breaking events; micro–scale, spilling and plunging. The three types are fairly easily separated. Typical examples are seen in Figure 2. Two independent observers of the video record agreed on the classification of the breaking events into these three categories with insignificant deviations. For the event to be counted in the video record it had to occur within a 0.1 *m* radius of the penetration of the wave wire through the mean water level.

For the wave breaking analysis, wave wire data were processed to obtain a time series of the spectral energy density, E_{6-10}, in the frequency band 6–10 *Hz* with a sampling interval of 1/8 second (see Ataktürk, 1991). In our previous study (Weissman et al., 1984) we had devised a technique to detect the breaking events from such a time series by using the breaking criteria: (i) the spectral energy in a

high frequency band exceeds a threshold, and (ii) the data point is in the crest region (i.e., in the vicinity of a local maximum). Since the threshold, i.e., the absolute value of the measured band energy varies with wind speed (stress), gustiness, underlying long waves, currents etc., it had to be determined individually for each run. In the current study, this difficulty was greatly reduced by defining a new detection parameter, N_σ, based on the fluctuating component of band energy normalized by its root–mean–square value;

$$N_\sigma = \frac{E_{6-10} - \overline{E}_{6-10}}{E_{\sigma,6-10}} \tag{3}$$

Table I: General description of the data sets analyzed. Duration of each run is two hours. For each run, the first row indicates the mean values and the second row the standard deviations.

Run#	Date Y/M/D	Time	U_{10N} (m/s)	u_* (m/s)	T_{s-10} (°C)	T_s (°C)	z/L	f_p (Hz)	H_s (m)	ak	$\frac{U_{10N}}{C_p}$
1100	86/8/25	15:32	4.35 0.38	0.16 0.02	−1.15 0.22	23.26 0.03	−0.27 0.04	0.67 0.04	0.13 0.02	0.09 0.01	1.88 0.23
1101	86/8/25	17:36	4.69 0.93	0.17 0.04	−1.18 0.31	23.13 0.11	−0.24 0.10	0.70 0.05	0.12 0.03	0.09 0.01	2.09 0.38
1102	86/8/26	11:20	4.21 0.34	0.15 0.01	−1.83 0.24	23.09 0.12	−0.21 0.03	0.75 0.09	0.09 0.01	0.08 0.01	2.01 0.32
1103	86/8/26	15:00	5.18 0.32	0.18 0.01	−2.70 0.42	23.78 0.06	−0.08 0.03	0.64 0.03	0.13 0.00	0.10 0.00	2.13 0.20
1104	86/8/27	12:03	3.36 0.83	0.12 0.03	−2.60 0.62	23.26 0.06	−0.25 0.21	0.70 0.05	0.10 0.02	0.07 0.01	1.51 0.37
1106	86/9/11	18:35	5.84 1.01	0.22 0.04	4.21 0.33	20.50 0.05	−0.44 0.29	0.55 0.02	0.18 0.02	0.12 0.01	2.05 0.31
1107	86/9/12	14:41	4.31 0.42	0.16 0.02	1.82 0.32	21.04 0.05	−0.56 0.13	0.66 0.07	0.13 0.01	0.10 0.01	1.81 0.27
1013	87/5/15	12:30	5.85 0.92	0.22 0.04	3.63 0.11	16.29 0.01	−0.34 0.16	0.55 0.02	0.19 0.02	0.12 0.01	2.05 0.32
1014	87/5/15	14:45	5.23 1.12	0.19 0.05	2.90 0.26	16.41 0.05	−0.44 0.25	0.59 0.04	0.17 0.03	0.11 0.01	1.96 0.35
89.10	89/7/19	17:05	6.83 0.55	0.26 0.02	1.09 0.18	22.06 0.18	−0.28 0.05	0.57 0.06	0.21 0.03	0.13 0.01	2.47 0.16

(a) micro–scale (b) spilling (c) plunging

Figure 2: The three types of wave breaking characterized from our video records.

where $\bar{E}_{6-10}$ and $E_{\sigma,6-10}$ respectively, are the mean and standard deviation of E_{6-10} calculated from a record typically 17 minutes in length. (Out of 66 records, two records were short – 8.5 minute in duration. The statistics from these runs were included by simply doubling the number of breaking events.) Also, data points within ±90° phase of the local maximum were considered to be *on the crest.*

Long wave spectra were calculated from the 17 min wave height records. An equivalent number of wave crests, N_{crest}, in the record was defined as the duration, T, times the frequency of the waves at the peak of the spectrum, f_p:

$$N_{crest} = T f_p \ . \tag{4}$$

From video records, N_{break}, number of crests on which breaking occurred, was found. Percentage of crests with breaking,

$$\%B = \frac{N_{break}}{N_{crest}} \times 100 \tag{5}$$

was initially calculated separately for the events of plunging, spilling and micro–scale breakers. Since the frequencies of occurrence of spilling and plunging breakers were about the same and the micro–scale breaking turned out to be ubiquitous and not well correlated with any turbulence or sea state measure, presentation of results has been done in terms of the sum of percentages of crests with breaking of type plungers and spillers, $\%B_{s+p}$.

In a separate study, Ataktürk (1991) has analyzed the wind stress measurements of the current study and additional data runs, and obtained the relationship between the drag coefficient and neutral 10 m mean wind speed valid for the fetch and water surface conditions at our Lake Washington site;

$$C_{DN} = (0.75 + 0.10U_{10N}) \times 10^{-3} \quad (6)$$

This formula was used with the Liu et al. (1979) formulation for calculating turbulent fluxes from mean atmospheric measurements. The calculation of wind stress or equivalently the friction velocity from mean wind speed with this numerical scheme includes corrections for the influence of atmospheric stratification.

We also determined the inverse wave age, U_{10N}/C_p or u_*/C_p, for each run, where $C_p = g/\omega_p$ is the phase speed of the dominant waves corresponding to the angular frequency, $\omega_p = 2\pi f_p$, of the spectral peak and, g is the acceleration due to gravity.

$\%B_{s+p}$ was correlated with various measures of the atmospheric turbulence and the *relative wind forcing* (identically equivalent to the inverse wave age). Both single and dual parameter linear regressions (Lapin, 1983) were calculated for several variables using the statistical program package *Quattro–Pro*. A curvilinear fit was also tried when it was noted that a linear fit for a certain variable was not optimal.

RESULTS

Figure 3a is a plot of $\%B$ determined from video records and separated into micro–scale, spilling and plunging types, versus U_{10N}. Micro–scale breaking occurs to about the same extent at all wind speeds, while spilling and plunging type breakers display a similar behaviour in frequency of occurrence which increases with increasing U_{10N}. Therefore, further analyses were carried only for the combined effects of spilling and plunging breakers.

Comparisons of simultaneous video and wave wire records showed that, in general, micro–scale breaking is associated with events for which $N_\sigma < 8$ and, spilling or plunging breaking may be characterized by $N_\sigma \geq 8$. Events with $N_\sigma \geq 12$ were always due to plungers. In Figure 3b, percentage of crests with spilling or plunging breaking, $\%B_{s+p}$, determined from video records and percentage of crests with events $N_\sigma \geq 8$ obtained from wave wire records are plotted as a function of U_{10N}. Although the distributions of the data points are similar, some differences in their magnitudes are visible: values from video records are smaller at low winds, and larger at high winds. These differences may result from, respectively, (i) sensitivity of wave wire to small scale features which may not be visible on video records, (ii) insensitivity of wave wire to events that occur nearby but do not directly touch the sensor. The latter may be improved by using an array of wave wires which would allow spatial averaging.

In the studies by Jessup et al. (1990, 1991a) and Bush et al. (1991) some spikes in the radar backscatter were found not to correspond to any visible breaking events. Those events may be carried by the

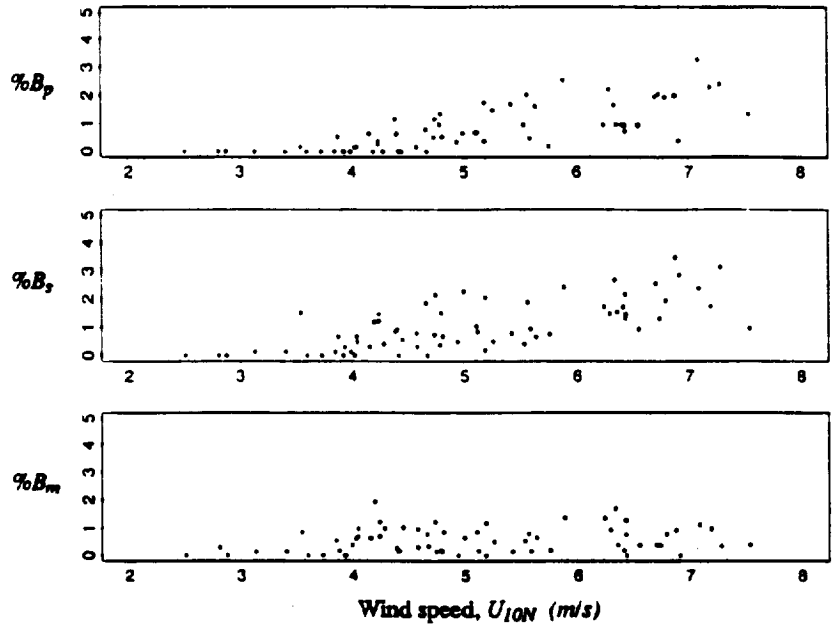

Figure 3a: Percentages of crests with micro-scale, $\%B_m$, spilling, $\%B_s$, or plunging, $\%B_p$, breaking versus wind speed, U_{10N}, determined from video records.

same features (for instance sharp corners) that cause N_σ to be large (but still $N_\sigma < 12$). This indicates that the radars are quite sensitive to such features, even if they do not cover the whole radar footprint.

Some of our $8 < N_\sigma < 12$ events (or perhaps even a few of the $N_\sigma > 12$ cases) correspond to strong Doppler shifts causing the amplitudes of the signals at 6–10 Hz to be increased (being that they are really due to surface features of much lower intrinsic frequency. See, for instance, Ataktürk and Katsaros (1987) for a discussion of Doppler shifts in wave wire data.).

Figure 4 shows the dependence of $\%B_{s+p}$ on Re, $U_{10}^{3.75}$, u_*/C_p and u_*^2. Reynolds number, Re, was defined as (Toba and Koga, 1986):

$$\mathrm{Re} = \frac{u_*^2}{\nu\omega_p} \tag{7}$$

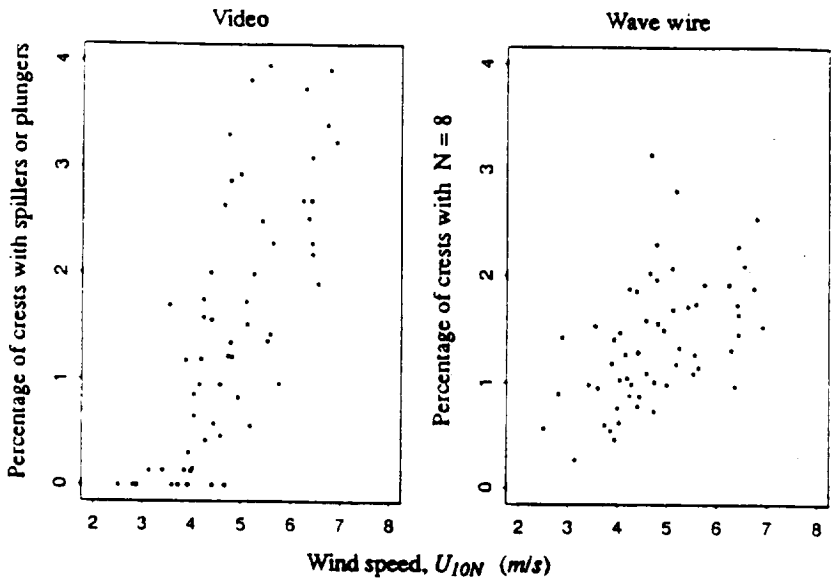

Figure 3b: Statistics of breaking events obtained from video and wave wire records versus wind speed, U_{10N}.

where ν is the kinematic viscosity of air. All these parameters are about equally good predictors of $\%B_{s+p}$. However, from the statistics of the regression analysis provided in Table II it is seen that u_*^2 which explains 62% of the variations in $\%B_{s+p}$, is the best one among the individual variables used. (Although $u_*^{1.6}$ gives a slightly better correlation, for the limited data set the difference is not significant.)

This point is further illustrated in Figure 5 of $\%B_{s+p}$ versus u_*/C_p where the data points have been stratified according to the values of u_*^2. There is obviously a dependence on both the value of u_*^2 and u_*/C_p. Even though the two measures are not independent (since both contain u_*), it makes sense to examine for a certain wave age the variability in the $\%B_{s+p}$ as a function of wind stress (here calculated from U_{10N}). The regression lines show that for strong relative wind forcing (large inverse wave age), the increase in $\%B_{s+p}$ as a function of u_*/C_p is greater for large values of u_*^2. Also, from Table II it is seen that the pair, u_*^2 and u_*/C_p, explains a higher proportion of the variance of $\%B_{s+p}$ than u_*^2 alone with a proportional reduction of 11% in the previously unexplained variation.

Multiple regressions using (u_*^2, Re) or $(u_*^2, Re, u_*/C_p)$ produced still better statistical results by explaining, respectively, 69% and 72% of the variance of $\%B_{s+p}$. However, physical interpretations of

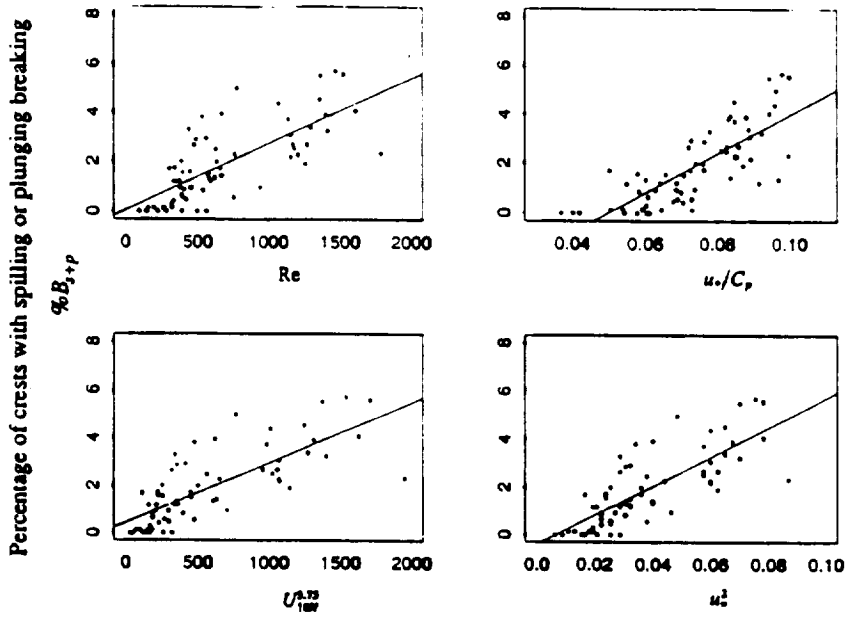

Figure 4: Linear regressions of $\%B_{s+p}$ for various predictors. A summary of the statistics obtained from regression analysis is provided in Table II.

Table II: Summary of the statistics obtained from regression analysis. The analyses were carried out following the definitions in Lapin (1983). Square–root of the *3rd* column is the correlation coefficient.

Regression	Standard Error of Estimate	Sample Coefficient of Determination
$\%B_{s+p} = 0.03 + 2.68 \times 10^{-3} Re$	1.07	0.54
$\%B_{s+p} = 0.44 + 2.52 \times 10^{-3} U_{10N}^{3.75}$	1.02	0.58
$\%B_{s+p} = -3.97 + 79.48\, u_*/C_p$	0.99	0.60
$\%B_{s+p} = -0.41 + 61.09\, u_*^2$	0.99	0.62
$\%B_{s+p} = -2.47 + 32.87\, u_*^2 + 42.37 u_*/C_p$	0.93	0.66

such combinations of variables are not as clear to us (but see Toba and Koga (1986)). Also, in view of the large scatter, it does not make sense to try very complicated functional forms until a greater data base has been formed or a convincing physical relationship has been proposed. Therefore, these results are not included in Table II.

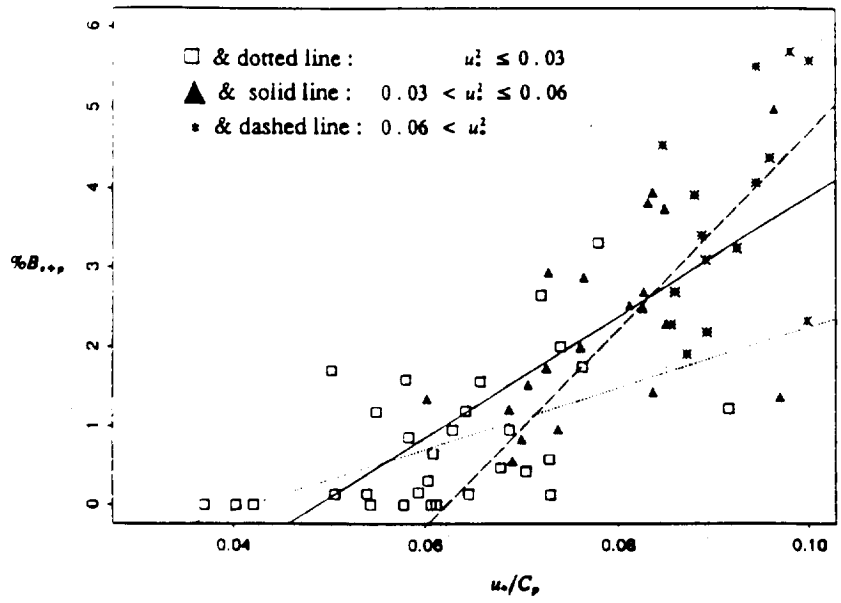

Figure 5: Percentage of crests with spilling or plunging breakers, $\%B_{s+p}$, versus u_*/C_p. For three ranges of u_*^2 separate symbols and linear fits have been used, as indicated on the figure.

DISCUSSIONS

Predictability of the percentage of crests with spilling or plunging breakers, $\%B_{s+p}$, were investigated using a set of variables, Re, $U_{10}^{3.75}$, u_*/C_p and u_*^2. These variables were chosen because such correlations make sense from a physical point of view. (For interpretations of the first two variables, see Toba and Koga (1986) and Wu (1979), respectively). In Table II we note that the highest sample coefficient of determination and the minimum standard error are obtained for the regression of $\%B_{s+p}$ as a function of u_*^2 and u_*/C_p. This result implies that for wave breaking both the magnitude of the wind stress and the degree of evolution of the surface waves are important.

It is easy to understand that young waves which are being strongly forced by a large wind stress should be breaking more frequently. Whether young waves, which are also short (i.e., the wavelength at the peak of the spectrum is short) break more frequently than those that have a wider spectral range through which to distribute the wind input by non–linear interactions – we intend to inves-

tigate further. We hypothesize that the absolute width of the wave spectrum (or the value of the wave number at the peak of the spectrum) could be considered as another parameter for improving the prediction of the incidence of wave breaking.

Jessup et al. (1990) suggested that the information content of the frequency of spikes in the radar cross section may also be used to study the variability of wave breaking. We suggest that the band passed data from an array of simple wave gauge wires may serve the same purpose. Since we have seen that $N_\sigma \gg 12$ consistently corresponds to visible breaking in all our wind wave records, this characteristic can now be used to count breaking waves. Enough cases can then be added by objective analysis to establish statistically significant information about the dissipation of surface waves under various forcing conditions as determined by wind stress and relative wind stress forcing. We are currently adding more cases on the breaking of pure wind waves on Lake Washington from two more summer seasons.

Once the interrelationships have been established for the simple case of wind driven waves, the role and importance of swell (of variable amplitude and relative direction to the wind waves) as well as surface currents in wave breaking can then be studied more effectively.

Acknowledgements: We would like to thank Mr. Ralph C. Monis who spent countless hours watching the video records for detection and classification of breaking events and assisted in data processing. This study was supported by the *National Aeronautics and Space Administration* under Grant *NAGW–1322*.

REFERENCES

Ataktürk , S.S., 1991: Characterization of roughness elements on a water surface. Ph.D. Dissertation, Department of Atmospheric Sciences, University of Washington, Seattle, WA, 98195, 196 pp.

Ataktürk , S.S. and K.B. Katsaros, 1987: Intrinsic frequency spectra of short gravity–capillary waves obtained from temporal measurements of wave heights on a lake. *J. Geophys. Res.*, 92, 5131–5141.

Banner, M.L., 1990: The influence of wave breaking on the surface pressure distribution in wind–wave interactions. *J. Fluid Mech.*, 211, 463–495.

Banner, M.L. and E.H. Fooks, 1985: On the microwave reflectivity of small–scale breaking water waves. *Proc. R. Soc. Lond.*, A 211, 93–109.

Bush, D.A., S.P. Gogineni, R.K. Moore, K.B. Katsaros, and S.S. Ataktürk, 1991: A video–aided study of sea spikes in radar backscatter at moderate incidence. (Manuscript submitted to *IEEE Trans.*)

Hasselmann, S., K. Hasselman, L.H. Allender, and T.P. Barnett, 1985: Computations and parameterizations of the nonlinear energy transfer in a gravity–wave spectrum. Part II: Parameterizations of the nonlinear transfer for applications in wave models. *J. Phys. Oceanogr.*, 15, 1378–1391.

Jessup, A.T., W.C. Keller, and W.K. Melville, 1990: Measurements of sea spikes in microwave backscatter at moderate incidence. *J. Geophys. Res.*, 95, 9679–9688.

Jessup, A.T., W.K. Melville, and W.C. Keller, 1991a: Breaking waves producing sea spikes in microwave backscatter. Part II: Dependence on wind and wave conditions. (To appear in *J. Geophys. Res.*)

Jessup, A.T., W.K. Melville, and W.C. Keller, 1991b: Breaking waves producing sea spikes in microwave backscatter. Part I: Detection and visual verification. (To appear in *J. Geophys. Res.*)

Komen, G.J., S. Hasselmann, and K. Hasselmann, 1984: On the existence of a fully developed wind–sea spectrum. *J. Phys. Oceanogr.*, 14, 1271–1285.

Lapin, L.L., 1983: *Probability and Statistics for Modern Engineering*. PWS Publishers, B/C Engineering Division, Boston, MA, 624 pp.

Liu, W.T., K.B. Katsaros and J.A. Businger, 1979: Bulk parameterization of air–sea exchanges of heat and water vapor including the molecular constraints at the interface. *J. Atmos. Sci.*, 36, 1722–1735.

Monahan, E.C., 1968: Sea spray as a function of low elevation wind speed. *J. Geophys. Res.*, 73, 1127–1137.

Monahan, E.C., 1971: Oceanic whitecaps. *J. Phys. Oceanogr.*, 1, 139–144.

Monahan, E.C. and I.G. O'Muircheartaigh, 1980: Optimal power–law description of oceanic whitecap coverage dependence on wind speed. *J. Phys. Oceanogr.*, 10, 2094–2099.

Monahan, E.C., D.E. Spiel and K.L. Davidson, 1983: Model of Marine Aerosol Generation via Whitecap and Wave Disruption. *Ninth Conference Aerospace and Aeronautical Meteorol., Am. Meteorol. Soc.*, pp. 147–152.

O'Muircheartaigh, I.G. and E.C. Monahan, 1986: Statistical aspects of the relationship between oceanic whitecap coverage wind speed and other environmental factors. In *Oceanic Whitecaps*, E.C. Monahan and G.M. Niocaill, Eds., D. Reidelberg Publishing Company, pp. 125–128.

O'Muircheartaigh, I.G., M. Claffey, and E.C. Monahan, 1991: Modeling the wind–dependence of whitecapping using hierarchical models and parametric empirical Bayes methodology. Presented in *XX General Assembly of the IUGG*, 11–24 August, 1991, Vienna, Austria.

Phillips, O.M., 1988: Radar returns from the sea surface–Bragg scattering and breaking waves. *J. Phys. Oceanogr.*, **18**, 1065–1074.

Smith, S.D., 1980: Wind stress and heat flux over the ocean in gale–force winds. *J. Phys. Oceanogr.*, **10**, 709–726.

Snyder, R.L., F.W. Dobson, J.A. Elliott, and R.B. Long, 1981: Array measurements of atmospheric pressure fluctuations above surface gravity waves. *J. Fluid Mech.*, **102**, 1–59.

The WAMDI Group; S. Hasselmann, K. Hasselmann, E. Bauer, P.A.E.M. Janssen, G.J. Komen, L. Bertotti, P. Lionello, A. Guillaume, V.C. Cardone, J.A. Greenwood, M. Reistadt, L. Zambresky, and J.A. Ewing, 1988: The WAM model–A third generation ocean wave prediction model. *J. Phys. Oceanogr.*, **18**, 1775–1810.

Toba, Y. and M. Koga, 1986: A parameter describing overall conditions of wave breaking, whitecapping, sea–spray production and wind stress. In *Oceanic Whitecaps*, E.C. Monahan and G.M. Niocaill, Eds., D. Reidelberg Publishing Company, pp. 37–47.

Weissman, M. A., K. B. Katsaros, and S.S. Ataktürk, 1984: Detection of breaking events in a wind–generated wave field. *J. Phys. Oceanogr.*, **14**, 1608–1619.

Wu, J., 1979: Oceanic whitecaps and sea state. *J. Phys. Oceanogr.*, **7**, 1064–1068.

Wu, J., 1986: Whitecaps, bubbles, and spray. In *Oceanic Whitecaps*, E.C. Monahan and G.M. Niocaill, Eds., D. Reidelberg Publishing Company, pp. 113–124.